AAPS PharmSciTech (2024) 25:216
https://doi.org/10.1208/s12249-024-02930-7

RESEARCH ARTICLE

PEGylated pH-Responsive Liposomes for Enhancing the Intracellular Uptake and Cytotoxicity of Paclitaxel in MCF-7 Breast Cancer Cells

Harsh P. Nijhawan[1] · Pooja Shyamsundar[1] · Bala Prabhakar[1] · Khushwant S. Yadav[1]

Received: 30 March 2024 / Accepted: 3 September 2024

Abstract

This study aimed to develop paclitaxel (PTX)-loaded PEGylated (PEG)-pH-sensitive (SpH) liposomes to enhance drug delivery efficiency and cytotoxicity against MCF-7 breast cancer cells. PTX-loaded PEG-SpH liposomes were prepared using the thin film hydration method. ATR-FTIR compatibility studies revealed no significant interactions among liposome formulation components. TEM images confirmed spherical morphology, stability, and an ideal size range (180–200 nm) for improved blood circulation. At pH 5.5, liposomes exhibited increased size and positive zeta potential, indicating pH-sensitive properties due to CHEMS response to the acidic tumor microenvironment. Conversely, at pH 7.4, liposomes showed a slightly larger size (199.25 ± 1.64 nm) and a more negative zeta potential (-36.94 ± 0.32 mV), suggesting successful PEG-SpH surface modification, enhancing stability, and reducing aggregation. PTX-loaded PEG-SpH liposomes demonstrated high encapsulation efficiency (84.57 ± 0.92% w/w) and drug loading capacity (4.12 ± 0.26% w/w). *In-vitro* drug release studies revealed accelerated first-order PTX release at pH 5.5 and a controlled zero-order release at pH 7.4. Cellular uptake studies on MCF-7 cells demonstrated enhanced PTX uptake, attributed to mPEG-PCL incorporation prolonging circulation time and CHEMS facilitating PTX release in the tumor microenvironment. Furthermore, PTX-loaded PEG-SpH liposomes exhibited significantly improved cytotoxicity with an IC_{50} value of 1.107 µM after 72-h incubation, approximately 90% lower than plain PTX solution. Stability studies confirmed the robustness of the liposomal formulation under various storage conditions. These findings highlight the potential of PEGylated pH-responsive liposomes as effective nanocarriers for enhancing PTX therapy against breast cancer.

Keywords paclitaxel · MPEG-PCL · PH-sensitive · liposomes · CHEMS · MCF-7 cells

Introduction

Breast cancer remains a formidable global health challenge, particularly affecting women and posing a significant risk of mortality. It is characterized by irregular cell proliferation within breast tissues, primarily occurring in the inner lining of the milk ducts or the glands responsible for milk production. In light of recent statistics, the American Cancer Society (ACS) estimates that in the current year, there will be 297,790 new cases of invasive breast cancer diagnosed in women and 2,800 new cases in men [1]. Additionally, 55,720 new cases of ductal carcinoma *in situ* (DCIS) will be diagnosed [2]. In the United States, it is estimated that one in every eight women will be diagnosed with breast cancer at some point during her lifetime [1]. Even though surgery is the recommended treatment for removing breast cancer, it is very challenging to remove the tumor and prevent its recurrence entirely. Thus, chemotherapy is needed to compensate for the surgical shortfall.

Taxanes are a class of chemotherapeutic drugs that have been proven to be a feasible therapeutic option for breast cancer [3]. Paclitaxel (PTX) is a natural product extracted from the bark of Taxus brevifolia with effective chemotherapeutic activity [4]. It has significant tumoricidal ability against breast, ovarian, non-small cell lung, neck cancer, and AIDS-related Kaposi's Sarcoma [5]. It affects the enhancement of cell tubulin polymerization and the inhibition of M-phase. As PTX is insoluble in water, its marketed formulation, Taxol®, is prepared using Cremophor® EL (polyethoxylated castor) and ethanol [6]. Despite several dilutions

✉ Khushwant S. Yadav
khush.yadav@gmail.com; Khushwant.Yadav@nmims.edu

[1] Shobhaben Pratapbhai Patel School of Pharmacy & Technology Management, SVKM's NMIMS (Deemed to Be University), Mumbai, India

Published online: 17 September 2024

before use, hypersensitivity is reported due to the higher amount of Cremophor® EL required to deliver the drug [7]. These rules out Cremophor® EL, thus paving the way for the need for a promising approach with good biocompatibility and low toxicity.

Nanotechnology has emerged as a promising frontier in cancer therapeutics, potentially mitigating systemic toxicity while enhancing therapeutic efficacy [8–10]. Among various nanocarriers, liposomes have garnered significant attention for drug delivery due to their versatility and biocompatibility [11, 12]. Liposomes, comprising lipid bilayers encapsulating hydrophilic and lipophilic drugs, exhibit similarities to biological membranes, providing enhanced stability and prolonged circulation times in the bloodstream [13]. However, their rapid reticuloendothelial system (RES) clearance limits their accumulation in the target tumor tissues, thus necessitating strategies to prolong the circulation time and enhance tumor targeting [13, 14]. Surface modification utilizing polyethylene glycol (PEG) [15] or methoxy polyethylene glycol-polycaprolactone (mPEG-PCL) [16] has emerged as a pivotal strategy to overcome this challenge, leading to the development of long-circulating or "PEGylated" liposomes with improved pharmacokinetic profiles [17]. The hydrophilic PEG moiety forms a protective layer around the liposomes, mitigating opsonization and clearance by RES [18], thereby extending their circulation time. Meanwhile, the hydrophobic PCL segment integrates into the lipid bilayer, enhancing its structural integrity and stability.

Moreover, many strategies have been developed to improve the specificity of anticancer therapeutics toward tumor cells and tissues, whilst reducing adverse effects on surrounding healthy tissues [19, 20]. One of the promising strategies to enhance the liposomal drug delivery for breast cancer therapy involves leveraging the distinctive attributes of the tumor microenvironment, particularly its acidic environment pH [21]. The pH-sensitive liposomal drug delivery could offer a potential and versatile carrier for precise drug release within the tumor cells, thus enhancing the therapeutic effectiveness while minimizing the unintended effects on healthy tissues [22]. Cholesteryl hemisuccinate (CHEMS), an acid-sensitive ester derivative of cholesterol in the 3-hydroxyl group, is commonly utilized in pH-responsive liposomal formulations [23, 24]. These SpH liposomes remain stable at physiological pH (7.4) but exhibit controlled fusion with endosomal membranes, leading to rapid destabilization in acidic conditions such as those found in endosomes (pH 5.5) [22, 25, 26]. The integration of pH sensitivity along with mPEG-PCL further enhances liposomal formulations' efficacy, stability, circulation duration, and tumor-targeting capabilities [27]. Moreover, mPEG-PCL contributes to the stability of CHEMS within liposomes by establishing hydrophobic interactions with the lipid bilayer. This interaction prevents premature leakage, ensuring controlled drug release specifically within the acidic tumor microenvironment [28]. This improved stability significantly enhances the overall efficacy of the liposomal formulation, offering a more reliable and efficient delivery system for anticancer agents such as PTX.

In our previous study, we demonstrated the role of PEGylation using mPEG-PCL block co-polymer in enhancing the circulation and bioavailability of the drug. In this study, we aimed to examine the synergistic effects of PEGylated pH-sensitive (PEG-SpH) liposomes containing CHEMS and a synthesized mPEG-PCL copolymer moiety for enhancing the intracellular delivery of PTX in MCF-7 breast cancer cells. Herein, the mPEG-PCL copolymer was synthesized using a ring-opening polymerization technique and combined with SpH liposomes. The formulated PEG-SpH liposomes were then characterized for their physiochemical properties and the effect of different pH on particle size and zeta potential was evaluated. It was hypothesized that the presence of CHEMS would lead to lipid protonation and rapid destabilizing of PTX-loaded PEG-SpH liposome membrane in a tumor acidic environment, thereby leading to accelerated drug release, enhanced cellular uptake, and significantly improved cytotoxic activity of PTX against MCF-7 breast cancer cells. Therefore, these PEG-SpH liposomes show significant potential for breast cancer therapy, offering targeted delivery as well as cytosolic release of encapsulated anticancer drugs.

Materials and Methods

Materials

Paclitaxel (PXL) was generously provided as a gift sample from Cipla (Mumbai, India). Leciva S-90 was also kindly gifted by VAV Lipids (Mumbai, India). Cholesterol (97% purity) and chloroform were procured from Loba Chemie Pvt. Ltd, (Mumbai, India). Poly (ε-caprolactone), monomethoxy poly (ethylene glycol), cholesteryl hemisuccinate (CHEMS), methyl ether, and stannous octoate were obtained from Sigma Aldrich, (Mumbai, India). Dichloromethane (DCM), oleic acid, petroleum ether, and methanol were obtained from Research labs (Mumbai, India). All water used in the experimental studies was Millipore-Q ultrapure water. All the other chemicals and reagents used were of analytical grade.

Synthesis and Characterization of mPEG-PCL Copolymer

The mPEG-PCL copolymer was synthesized using the ring-opening polymerization method following our previously

published work [16]. Briefly, 7 g of PCL (Mn = 45,000) and 7 g of mPEG (Mn = 5000) in the ratio 1:1 was added to a three-necked round bottom flask (RBF) with 4–5 drops of stannous octoate (0.01 mmol) acting as the reaction catalyst under a dry nitrogen atmosphere. The assembly was stirred for 6 h at 110°C. Later, the mixture was de-gassed using nitrogen for approximately 30 min and allowed to cool at room temperature. Further, the mixture was dissolved in DCM and precipitated using an excess of cold petroleum ether [16]. The copolymer formed was filtered, dried at room temperature, and stored in an airtight container. The synthesized mPEG-PCL copolymer was then characterized using Nuclear Magnetic Resonance (NMR) spectroscopy with a SpinSolve 60 instrument (Magritek, Germany) [29]. This NMR analysis conformed structural integrity and composition of the co-polymer. Furthermore, it was then subjected to Fourier Transform Infrared Spectroscopy (FTIR) using a Perkin Elmer, Spectrometer (Spectrum Two). Accurately weighed mPEG-PCL copolymer samples were placed on the cleaned diamond surface of the spectrometer and the spectroscopy was performed within the frequency range of 4000 to 400 cm^{-1} [16].

Preparation of PTX-loaded SpH Liposomes

PTX-loaded SpH liposomes were prepared using the thin film hydration method [13] with slight modifications. Briefly, paclitaxel (10 mg), cholesterol (10 mg), Leciva S-90 (180 mg), and CHEMS (4 mg), (molar ratio of 12:26:228:8) were taken in an RBF and dissolved in an organic solvent mixture of chloroform: methanol (2:1 ratio v/v) [30]. The organic solvent was flash evaporated by attaching the RBF to a rotary evaporator (IKA, RV 10) with an attached water bath at 60°C, 25 mmHg vacuum, and 100 rpm to form a thin film. The deposited film was further nitrogen stream dried for 1 h and vacuum desiccated for 2.5 h. The obtained dried thin film was then hydrated using 10 mL of phosphate buffer saline (PBS) pH 7.4 and 1–2 drops of surfactant oleic acid for 24 h and at 8°C. The liposomal suspension thus formed was subjected to size reduction by probe sonication (Sonics model VCX-130) at 40% amplitude and 2-s on and 2-s off pulse mode over an ice bath. The blank liposomes (without PTX) were prepared as described earlier.

Preparation of PTX-Loaded PEG-SpH Liposomes

The PTX-loaded PEG-SpH liposomes were prepared following a procedure similar to the one mentioned. In addition, an accurately weighed amount of previously prepared mPEG-PCL copolymer (10 mg) was added along with paclitaxel, cholesterol, Leciva S-90, and CHEMS in RBF and dissolved in an organic solvent mixture of chloroform: methanol (2:1 ratio v/v). All liposome preparations were stored in airtight containers at 4°C.

Characterization of PTX-Loaded PEG-SpH Liposomes

Drug Excipient Compatibility: ATR-FTIR Studies

Fourier Transform Infrared (FTIR) spectra were acquired using a UATR Two Perkin Elmer instrument (Perkin-Elmer, Inc, USA) equipped with attenuated total reflectance (ATR) capabilities [31]. Individual FTIR spectra were generated for pure PTX, Leciva S-90, cholesterol, CHEMS, mPEG-PCL, and PTX-loaded PEG-SpH liposomes, and subsequently compared. To ensure the measurements' reliability, the ATR-FTIR instrument's diamond surface was meticulously cleaned with carbon tetrachloride (CCl_4). Subsequently, 5 mg of each sample was positioned, and scans were conducted with torque gradually increased up to 70%. Automatic baseline corrections were applied using the accompanying software spectrum. The examined infrared spectral wavelength spanned from 4000 cm^{-1} to 400 cm^{-1}, with a spectral resolution of 4 cm^{-1} [16].

Surface Morphology Studies

The PTX-loaded PEG-SpH liposomes were visualized utilizing a Transmission Electron Microscope (TEM) (TEC-12, TECNAI G2 SPIRIT BIOTWIN) working at 100 kV. In a concise methodology, 50 µL of appropriately diluted liposome samples were applied to copper grids coated with carbon (Electron Microscopy Sciences, USA). After a 2-min adsorption period, the samples were gently dried using an infrared lamp for 5 min. For enhanced contrast and visualization, negative staining was performed by applying 5 µL of phosphotungstic acid to the samples for 25 s. Excess phosphotungstic acid was carefully removed using Whatman filter paper. This staining procedure was repeated, and the samples were allowed to air-dry for 2–3 min. The prepared grids, hosting the liposome samples, were meticulously positioned in the TEM instrument for imaging and analysis. The imaging process employed Olympus Soft Imaging Solutions VELETA CCD Camera, and subsequent analysis was conducted using Tecnai Imaging & Analysis software.

Particle size and Zeta Potential Analysis

The particle size and polydispersity index (PDI) for all liposome formulations were measured through dynamic light scattering (DLS) at 25°C and a consistent 90° angle, using the Nano-ZS zeta sizer (Malvern Instruments, UK) [31]. The zeta potential measurements were assessed employing DLS coupled with electrophoretic mobility on the aforementioned equipment.

Effect of pH on Particle Size and Zeta Potential

To investigate the impact of pH on particle size and zeta potential, the PTX-loaded liposomes and PEG-SpH liposome samples were subjected to dilution in four distinct freshly prepared PBS with a pH value of 7.4, and acetate buffer with a pH of 6.8, 5.5, 4.5 at 37 ± 0.5°C. At different intervals, portions of the samples were extracted and the average particle size was analyzed using a Nano-ZS zeta sizer (Malvern Instruments, UK) [31]. Likewise, alterations in the zeta potential of the liposomes under different pH conditions were also assessed.

Encapsulation Efficiency and Drug Loading Capacity

The encapsulation efficiency of the prepared PTX-loaded PEG-SpH liposomes was determined by subjecting the liposomal suspension to centrifugation at 30,000 rotations per minute (rpm) for 25 min at 4°C, employing a refrigerated centrifuge (Optima MAX-XP ultracentrifuge with TLS-55 rotor, Beckman Coulter, USA) [32]. Subsequently, the supernatant, containing the PTX not encapsulated within the liposomes, was carefully separated and passed through a 0.45 µm cellular membrane. It was appropriately diluted with PBS pH 7.4 and quantitatively analyzed using a UV–visible spectrophotometer (Shimadzu-1800) configured to operate at a wavelength of 231.4 nm. The drug loading capacity was calculated by subtracting the amount of free PTX in the supernatant from the total amount of PTX used in the formulation and expressing it as a percentage relative to the total mass of the PEG-SpH liposomes [33]. The percentage of encapsulation efficiency and drug loading capacity were calculated using the formula provided in Eq. 1 and Eq. 2 respectively.

$$\%\ Entrapment\ efficiency = \frac{Total\ amount\ of\ PTX\ added - Free\ PTX}{Total\ amount\ of\ PTX\ added} \quad (1)$$

$$\%\ Drug\ loading\ capacity = \frac{Total\ amount\ of\ PTX\ added - Free\ PTX}{Mass\ of\ PEG - Sph\ liposomes\ (mg)} \quad (2)$$

In-Vitro Drug Release Studies and Kinetic Modeling

The *in-vitro* release of PTX from PEG-SpH liposomes was evaluated using the dialysis bag method [34]. PTX was dissolved in dimethyl sulfoxide (DMSO) to prepare a PTX solution. Specifically, 10 mg of PTX was dissolved in 2 mL of DMSO. This PTX solution was used as a comparative reference against the PTX-loaded liposomes. In brief, a 10 mg PTX equivalent of the liposomal formulations was introduced into a dialysis bag with a molecular weight cutoff (MWCO) of 14,000 Daltons (Da), previously soaked in Milli Q water for approximately 24 h (h) [33]. The dialysis bag was carefully sealed at both ends for a secure enclosure. Subsequently, the sealed dialysis bag was immersed in 80 mL of two distinct release media: PBS with a pH of 7.4 and acetate buffer with a pH of 5.5. The experimental setup was maintained at a temperature of 37 ± 0.5°C with continuous magnetic stirring at 100 rpm [35]. At specific, time intervals over 8 consecutive days, aliquots were withdrawn from the dialysis bag. An equivalent volume of fresh new medium was introduced to replace the removed sample to maintain sink conditions. The aliquots were appropriately diluted and the PTX content was analyzed spectrophotometrically, with measurements taken at a fixed wavelength of 231.4 nm (pH 7.4) and 231.9 nm (pH 5.5), respectively. To comprehend the release mechanism of PTX from PEG-SpH liposomes, *in-vitro* drug release data was fitted into various kinetic models using MS Excel (Microsoft Corporation). The data was fitted into zero-order, first-order, Higuchi, and Korsmeyer-Peppas models [36]. The Korsmeyer-Peppas model was used to distinguish between the competing release mechanisms of case-II transport (relaxation-controlled release), non-Fickian release (anomalous transport), and Fickian release (diffusion-controlled release) [16, 37, 38]. The equation's "n value" designates the type of diffusional exponent, which helps describe the drug release mechanism, and the r^2 value indicates accuracy [39].

Quantitative Cellular Uptake Studies on MCF-7 Breast Cancer Cell Line

The PTX-loaded PEG-SpH liposomes were subjected to a microplate reader approach for quantitative assessment of cellular uptake [40]. In 6-well plates, MCF-7 cells were seeded at a density of 2×10^5 cells per well, and incubated for 24 h to promote cell adhesion. Following this, the cells were incubated for 4 h in fresh medium with both free PTX solution and the liposomal formulation (100 µl/ml). The adherent cells in the well plates were subjected to three washing cycles with 2 ml of chilled PBS pH of 7.4 and kept at 4°C after the treatment period. A cell lysis buffer containing 1% v/v Triton-X100 in PBS pH of 7.4 was used to lyse the cells. Centrifugation was performed on the resulting cell lysate for 20 min at 10,000 rpm and 4°C. The drug concentrations in the supernatants were thereafter determined using fluorescence spectrophotometry (FLUOstar, Biotron BMG, Germany), with 420 and 540 nm as the excitation and emission wavelengths, respectively.

In-vitro Cytotoxicity Studies on MCF-7 Breast Cancer Cell Line

The *in-vitro* cytotoxicity investigations were conducted with slight modifications based on our prior published

work [31, 41]. The assessment involved PTX-loaded PEG-SpH liposomes using the MTT [(3-(4,5-dimethylthiazol-2-yl)-2,5-diphenyl tetrazolium bromide)] assay on MCF-7 cell lines. The MCF-7 cells were cultured in Dulbecco's Modified Eagle Medium (DMEM) supplemented with 1 mM sodium pyruvate, 2 mM L-glutamine, 10% fetal bovine serum, 4500 mg/L glucose, and 1500 mg/L sodium bicarbonate. 100 µL MCF-7 cells were sown into each well of a 96-well plate (Corning Incorporated Life Sciences, Acton, MA, USA) at a density of 4231 cells/mL and the plates were incubated at 37 ± 0.5°C, 5% CO_2, 95% air and 100% relative humidity for 24 h before addition of samples [31]. The liposome samples were dissolved in dimethyl sulfoxide (DMSO) at a concentration of 1000 µg/ml and then stored frozen until required. At the time of sample addition, an aliquot of frozen concentrate was thawed and diluted to 0.25 µM, 0.5 µM, 1 µM, 2.5 µM, 5 µM, 10 µM, 25 µM, 40 µM, and 50 µM. Aliquots of these different dilutions were added to the appropriate well plates and were incubated for 72 h [42]. Then, the assay was concluded by adding 20 µL of MTT reagent (5 mg/mL), followed by another additional 24 h incubation (in a 5% CO2 atmosphere at 37 ± 0.5°C). After carefully extracting the supernatant, 200 µl of DMSO was incorporated to lyse the cells and dissolve the formazan needles that had formed [42]. Lastly, an automated microplate reader (Lab system Multiskan, Helsinki, Finland) was utilized to measure absorbance at 550 nm with a reference wavelength of 690 nm. By assessing the absorbance of the investigated liposome formulations to the absorbance of the control medium in three successive experiments, each with $n = 6$, the average percentage of cell viability was determined [31]. The cytotoxicity was evaluated after 24 h, 48 h, and 72 h of incubation. An estimate of the drug or liposome formulation concentration required for inhibiting cell proliferation by 50% (IC_{50}) was determined by plotting the percentage of cell growth inhibition against the concentration of the pure drug or liposome formulation [43].

Stability Studies

The formulated PTX-loaded PEG-SpH liposomes' stability was evaluated by preserving the samples for 4 weeks at three different temperatures; 2–4°C, 25°C, and 37 ± 0.5°C with 60% relative humidity (RH). The Liposome samples were retrieved at the end of each subsequent week, appropriately diluted with PBS pH 7.4, and subjected to analysis for particle size, PDI, and zeta potential using the Nano-ZS zeta sizer (Malvern Instruments, UK) [16]. Following the previously mentioned methodology, the percentage entrapment efficiency was determined using a UV–visible spectrophotometer (Shimadzu-1800).

Data Analysis and Statistical Evaluation

Every experiment was carried out in three sets, and unless specifically stated otherwise, the results were reported as the mean ± standard deviation. All data were evaluated by either unpaired Student's t-test or one-way ANOVA using GraphPad Prism software (Version 10.1 for Windows, GraphPad Software, CA, USA). Statistically significant disparities between two correlated parameters were detected for *p*-values below 0.05. Nonetheless, certain investigations have indicated even lower *p*-values, such as 0.01 or less, as elaborated respectively.

Results and Discussion

Synthesis Formulation and Characterization of mPEG-PCL Copolymer

Ring-opening polymerization of PCL was employed to improve the synthesis of mPEG-PCL block copolymer by incorporating Sn (Oct)2 and mPEG into the reaction mixture. The NMR spectroscopy was employed to analyze the structure and composition of synthesized mPEG-PCL copolymer (Supplementary Fig. 1). The peaks at approximately 1.4 and 4 ppm can be attributed to the methylene protons in the PCL units [29]. Prominent peaks are observed between 3.7 and 3.5 ppm corresponding to the methylene and methoxy protons within the PEG units that constitute the co-polymer [29]. Additionally, lower intensity peaks in between 3 to 4 ppm are likely attributed to methylene protons in PEG end units that are connected to the PCL block [29]. The resulting FTIR spectrum for the mPEG-PCL block copolymer is depicted in Fig. 1. The discernible and intense bands observed at 1722.2 cm^{-1} and 1102.1 cm^{-1} can be attributed to the presence of carboxylic ester (C = O) and ether (C–O) groups, respectively [16]. The vibration bands caused by the asymmetric stretching of the C-H bond of methylene groups were depicted at 2885.4 cm^{-1} [44]. The peak at 1466.9 cm^{-1} indicated the twisting vibration of the same bonds. The signals in the spectrum matched with those seen in the same copolymers [44]. This observation signifies the successful synthesis of the mPEG-PCL copolymer.

Preliminary Batch Trials: Preparation of PTX-loaded PEG-SpH Liposomes

Initial preliminary batch trials were carried out to develop PTX-loaded PEG-SpH liposomes, keeping specific formulation factors consistent. PTX, lipid, cholesterol, and CHEMS were dissolved in methanol and chloroform, individually or in various ratios of 1:2, 1:1, and 2:1 v/v. A solvent blend of methanol and chloroform in a 2:1 v/v ratio was chosen for its

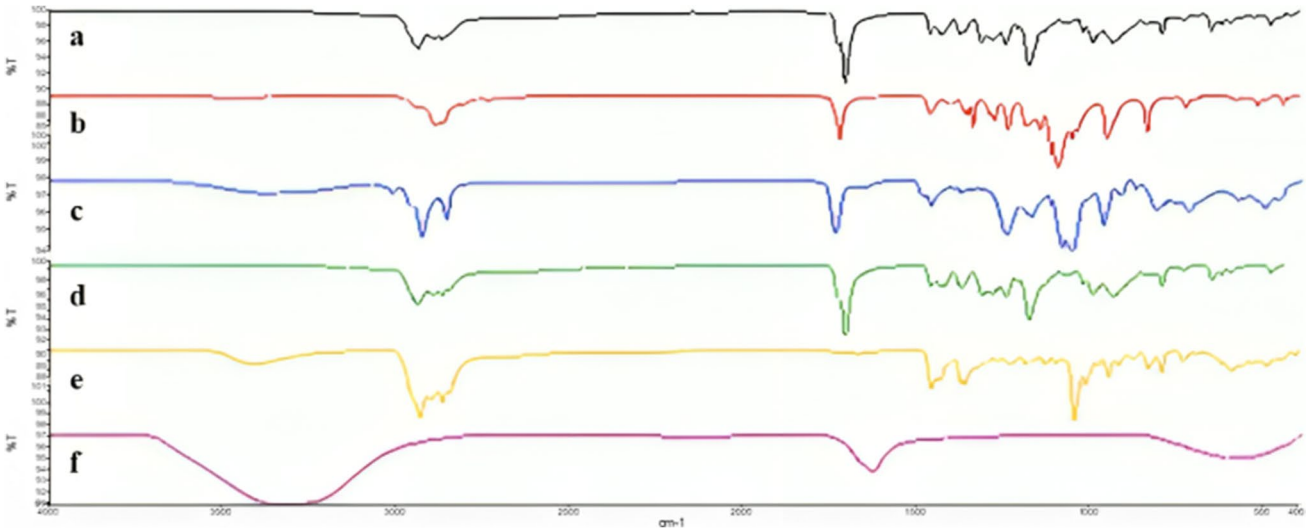

Fig. 1 ATR-FTIR spectra of **a** PTX, **b** Leciva S-90, **c** Leciva S-90, **d** Leciva S-90, **e** mPEG-PCL, **f** PTX-loaded PEG-SpH liposomes

superior solubility and film-forming properties. The formation of a uniform film was found to be influenced by several other variables, including the rotational speed, temperature of the water bath, and the size of the round-bottom flask. Through the use of a process of trial and error, optimization showed that using a flask with a bigger surface area and rotating it at 40°C and 100 rpm made the film form more consistently. After evaluating two size reduction methods—probe sonication and high-pressure homogenization—it was found that liposomes made with high-pressure homogenization had a lower entrapment efficiency (< 35%) and a higher polydispersity index (0.7–1) [45, 46]. For optimum liposome size reduction, the probe sonication method was chosen. An ice bath with a pulse mode 2 s on, 2 s off sonication cycle lasting 3 min was implemented to prevent formulation overheating during the size reduction process. The evaluation of encapsulation efficiency employed ultracentrifugation at 30,000 rpm for 25 min to ensure proper pellet and supernatant separation.

Characterization of PTX-Loaded PEG-SpH Liposomes

Drug-Excipient Compatibility: ATR-FTIR Studies

The ATR-FTIR spectra of a) PTX, b) mPEG-PCL, c) Leciva S-90, d) CHEMS, e) cholesterol, and f) PTX-loaded PEG-SpH liposomes are depicted in Fig. 1. The PTX spectra showed the characteristic band for C-H stretching (2935 cm^{-1}), C = O stretching (1707.7 cm^{-1}), and C–C stretching (1645 cm^{-1}) [47]. The mPEG-PCL copolymer spectra showed characteristic bands at 1722.2 cm^{-1} for C = O, 1102.1 cm^{-1} for C-O, 2885.4 cm^{-1} for C-H stretching, and 1466.9 cm^{-1} for twisting vibrations of C-H bending [15, 45, 46]. The characteristic C-H Stretching (Alkyl chain CH_3 and CH_2 stretching) of CHEMS can be seen between 2950–2850 cm^{-1} [48]. The absence of the characteristic PTX peak at 2935 cm^{-1} with the decrease and shift of peak at 1707.7 cm^{-1} demonstrates good encapsulation of PTX in PEG-SpH liposomes [49].

Surface Morphology Studies

The TEM images presented in Fig. 2 depict PTX-loaded PEG-SpH liposomes, showcasing their stability and structural integrity. These images highlight the vesicles' spherical morphology, indicating the absence of fusion or aggregation [50]. Such stability is essential for long-term performance, ensuring controlled drug release kinetics and prolonged circulation within biological systems [51]. Moreover, the size of liposome particles is critical in drug delivery, affecting permeability and retention. Studies have shown that liposomes ranging between 100 and 400 nm enhance retention and permeation, with particles smaller than 200 nm experiencing minimal clearance [52]. Notably, liposomes produced in our study fall within the size range of approximately 180–200 nm, aligning with the optimal range for improved blood circulation, penetration, and accumulation recommended for intravenous administration [53, 54].

Particle Size and Zeta Potential Analysis

This study examined the particle size and zeta potential of two distinct liposome formulations: PTX-loaded liposomes and PTX-loaded PEG-SpH liposomes. The summarized findings are presented in Table I. The PTX-loaded liposomes demonstrated a mean particle size of 185.46 ± 1.51 nm,

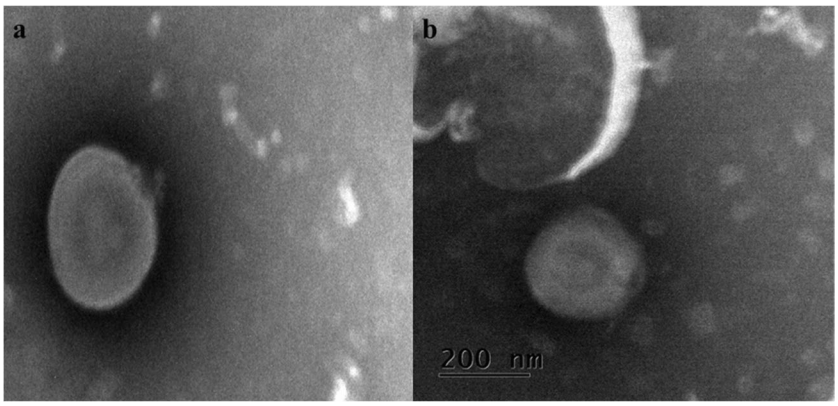

Fig. 2 Transmission electron microscopy (TEM) images of **a**, **b** PTX-loaded PEG-SpH liposomes. The scale bar represents 200 nm

Table I Characterization of Particle Size, Polydispersity Index (PDI), Zeta Potential, Encapsulation Efficiency, and Drug Loading Capacity for PTX-Loaded Liposomes and PEG-SpH Liposomes

Liposome formulation	Particle size (nm)	Polydispersity index (PDI)	Zeta potential (mV)	Encapsulation efficiency (%w/w)	Drug loading capacity (%w/w)
PTX-loaded liposomes	185.46 ± 1.51	0.17 ± 0.38	-28.91 ± 0.49	86.93 ± 0.73	4.34 ± 0.17
PTX-loaded PEG-SpH liposomes	199.25 ± 1.64	0.20 ± 0.75	-36.94 ± 0.32	84.57 ± 0.92	4.12 ± 0.26

accompanied by a low PDI of 0.17 ± 0.38. Furthermore, the zeta potential of PTX-loaded liposomes was measured at -28.91 ± 0.49 mV. Conversely, PTX-loaded PEG-SpH liposomes exhibited a slightly larger mean particle size of 199.25 ± 1.64 nm, with a marginally higher PDI of 0.20 ± 0.75. Notably, the zeta potential of PTX-loaded PEG-SpH liposomes was more negative compared to that of PTX-loaded liposomes, with a value of -36.94 ± 0.32 mV. The particle size of liposomes is a critical determinant affecting their pharmacokinetics and biodistribution, with smaller sizes typically favored for enhanced cellular uptake and tissue penetration [55]. The slight increase in particle size observed in PTX-loaded PEG-SpH liposomes may be attributed to PEGylation, provided by mPEG-PCL moiety, potentially resulting in augmented steric hindrance and consequently larger liposomes. Furthermore, the zeta potential of liposomes reflects their surface charge, crucial for stability and interaction with biological systems. The high negative zeta potential seen in PTX-loaded PEG-SpH liposomes, compared to PTX-loaded liposomes, could again be due to the presence of mPEG-PCL, facilitating increased repulsive forces between particles, and thereby enhancing stability.

Effect of pH on Particle Size and Zeta Potential

The effect of pH on the particle size and zeta potential of PTX-loaded liposomes and PTX-loaded PEG-SpH liposomes was investigated to understand the influence of pH on the stability and surface charge of the liposomal formulations. At physiological pH (7.4), PTX-loaded PEG-SpH liposomes demonstrated a particle size of 199.25 nm, compared to PTX-loaded liposomes with a particle size of 185.46 nm (Fig. 3a). This difference can be attributed to the surface modification with PEG-SpH, which enhances colloidal stability and mitigates particle aggregation. The presence of PEG chains on the liposome surface creates steric hindrance, preventing particle interactions and maintaining a smaller particle size [56]. However, as the pH decreases (at pH 5.5 and 4.4), a significant increase (p-value < 0.001 at pH 4.4 and p-value < 0.01 at pH 5.5) in the particle size of PTX-loaded PEG-SpH liposomes was observed. This pH-dependent increase in particle size suggests the influence of pH-sensitive properties conferred by the incorporation of pH-responsive moieties, such as CHEMS, in our liposomal formulation. The CHEMS likely undergo conformational changes or structural alterations in response to acidic pH, leading to particle swelling or fusion, and consequently, an increase in particle size [57, 58]. As the pH decreased from 7.4 to 4.5, there was a decrease in zeta potential values for PTX-loaded liposomes. This decrease in the zeta potential implies a transition towards a more positive surface charge, potentially arising from the protonation of negatively charged groups on the liposome surface under acidic conditions [59] (Fig. 3b). Conversely, PTX-loaded PEG-SpH liposomes demonstrated distinct pH-dependent characteristics. At pH 7.4, these liposomes exhibited a significantly more negative zeta potential of -36.94 mV compared to PTX-loaded liposomes, which showed a zeta potential of -28.91 mV, indicating effective surface

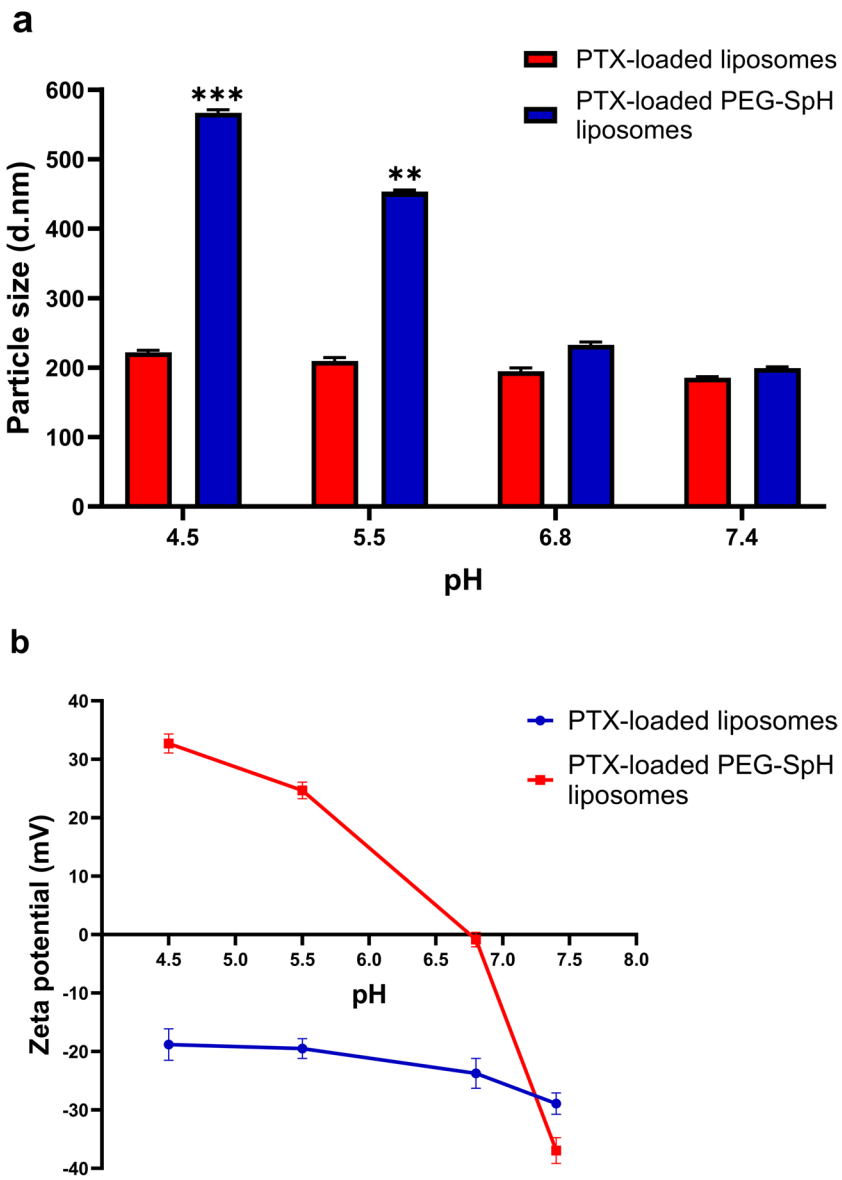

Fig. 3 pH-Dependent Change in **a** Particle Size and **b** Zeta Potential of PTX-Loaded PEG-SpH Liposomes. Data Represented as Mean ± SD ($n = 3$). (*** p-value < 0.001, ** p-value < 0.01 when Compared with PTX-Loaded Liposomes)

modification with PEG-SpH [16]. The incorporation of PEG-SpH likely introduced additional negatively charged groups on the liposome surface, leading to the observed increase in negative zeta potential. Interestingly, as the pH decreased, PTX-loaded PEG-SpH liposomes showed a gradual shift towards positive zeta potential values, eventually becoming positive with a zeta potential value of 32.70 mV at pH 4.5. This change in zeta potential directionality suggests a dynamic response to acidic pH conditions, possibly due to the protonation or alteration of pH-sensitive components within the liposomal membrane [60] and leading to the breakage of the bond between mPEG-PCL and Leciva S-90. The incorporation of CHEMS in our formulation was intended to impart pH sensitivity, allowing for a tailored response to acidic environments typical of tumor microenvironments.

Encapsulation Efficiency and Drug Loading Capacity

For PTX-loaded liposomes, the encapsulation efficiency was measured to be 86.93 ± 0.73% w/w, while the drug loading capacity was determined to be 4.34 ± 0.17% w/w. Conversely, PTX-loaded PEG-SpH liposomes exhibited slightly lower values for both encapsulation efficiency (84.57 ± 0.92% w/w) and drug loading capacity (4.12 ± 0.26% w/w) (Table I). High encapsulation efficiency in PTX-loaded liposomes and PTX-loaded PEG-SpH liposomes suggests effective PTX entrapment. Yet, the marginal decrease in efficiency in PEG-SpH liposomes may arise from interactions between PTX and PEGylated lipids, influencing lipid packing and PTX distribution within the liposomal carriers. Additionally, the role of Leciva S-90 concentration and cholesterol in influencing lipid bilayer

packing and drug encapsulation should be considered for improved formulation strategies.

In-vitro Drug Release Studies and Kinetic Modeling

In this study, the release profiles of PTX from three different formulations, PTX-solution, PTX-loaded liposomes, and PTX-loaded PEG-SpH liposomes, were evaluated under conditions mimicking physiological pH (7.4) and endosomal pH (5.5) as illustrated in Fig. 4. Firstly, for the PTX-solution, at pH 7.4, the release profile demonstrated rapid release, with 44.51% released within the first 1 h, escalating to 93.66% by the end of 8 h. Similarly, at pH 5.5, PTX release commenced rapidly, with 49.77% released within 1 h, and reaching 96.86% release at 8 h. The slightly higher release of PTX observed at pH 5.5 compared to pH 7.4 can be attributed to the acidic environment enhancing the solubility of PTX, resulting in increased PTX dissolution. For PTX-loaded liposomes, distinct release profiles were observed at pH 7.4 and pH 5.5, reflecting differences in drug release kinetics influenced by the surrounding pH environment. At pH 7.4, PTX release from liposomes was relatively slower, with 10.77% released within the first 15 min, gradually escalating to 79.36% release by 24 h. In contrast, at pH 5.5, PTX release commenced more rapidly, with 11.36% released within the initial 15 min, reaching 92.95% release by 36 h. Similar to the PTX solution, in the acidic pH (5.5), the liposomal membrane underwent structural changes or destabilization, leading to slightly higher release in comparison with pH 7.4 [25, 61]. For PTX-loaded PEG-SpH liposomes, the release profiles exhibited distinct patterns, showcasing the pH-responsive behavior of the formulation influenced by the presence of CHEMS. At pH 7.4, PTX release from PEG-SpH liposomes was relatively slower, with 33.61% released by the 30 min. The slower release of PTX from PEG-SpH liposomes at pH 7.4 can be attributed to the stabilized liposomal membrane at physiological pH, facilitated by the presence of deprotonated CHEMS that self-assembles into the lipid bilayers [62] and mPEG-PCL moiety [63], resulting in controlled drug release kinetics. Conversely, at pH 5.5, PTX release commenced more rapidly, with approximately half (52.62%) released within 30 min, and reaching 96.64% release by 36 h. The observed differences in release kinetics between pH 7.4 and 5.5 can be attributed to the pH-responsive properties conferred by CHEMS in the liposomal formulation. Under a physiological pH of 7.4, liposomes maintain their structural integrity owing to their negatively charged surface in the bloodstream. However, in the acidic tumor microenvironment pH (5.5), lipid protonation occurs, destabilizing the liposomes and thereby leading to accelerated drug release rates [64, 65]. CHEMS, with a carboxylic acid pK value of 5.8, ionizes at pH above 6, stabilizing lipid bilayers [66]. Conversely, below the pK value, acidic group deionization destabilizes the bilayer, resulting in increased drug release [67]. This smart behavior is attributed to CHEMS's ability to alter its molecular conformation and interact differently at various pH levels. In a similar study, Shah *et al*., 2022 formulated pH-sensitive liposomes using CHEMS to deliver an anticancer drug with a particle size of less than 200 nm. The use of CHEMS demonstrated tumor-responsive release, leading to enhanced cytotoxicity and cellular internalization of cisplatin [68].

The release kinetics of PTX-loaded liposomes and PTX-loaded PEG-SpH liposomes in pH 5.5 and 7.4 are summarized in Table II. At pH 5.5, both PTX-loaded liposomes

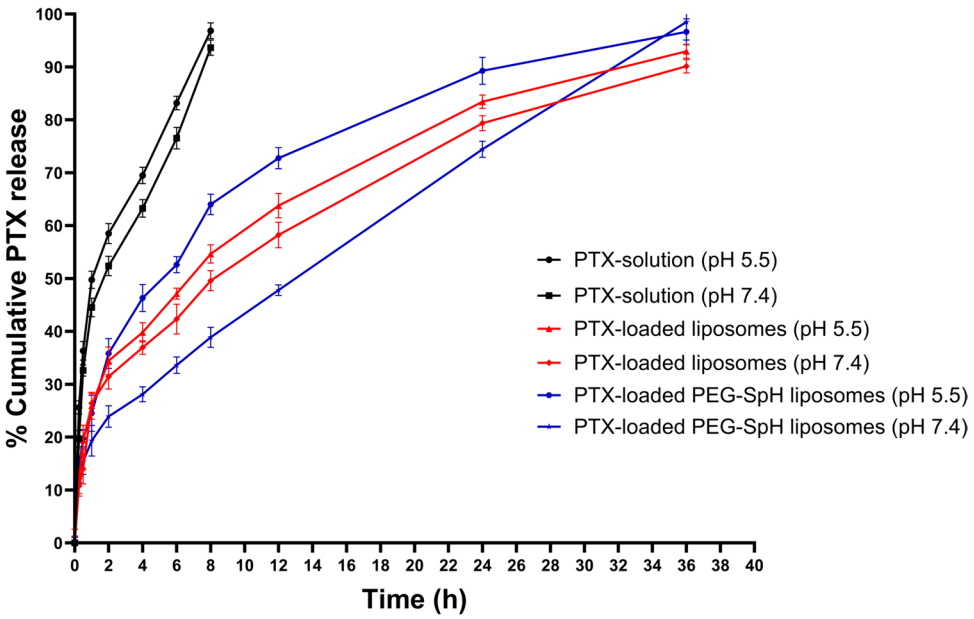

Fig. 4 *In-vitro* release behavior of PTX from PTX-loaded liposomes and PTX-loaded PEG-SpH liposomes evaluated under conditions mimicking physiological pH (7.4) and tumor acid environment pH (5.5). Data represented as mean ± SD ($n = 3$)

Table II Summary of Release Kinetics of PTX from PTX-Loaded Liposomes and PTX-Loaded PEG-SpH Liposomes in pH 5.5 and 7.4 According to Different Kinetic Models

Liposome formulation	Correlation coefficient (r^2) value of kinetic models			
	Zero-order	First order	Higuchi	Korsmeyer-Peppas
PTX-loaded liposomes (pH 5.5)	0.8747	0.9904	0.9846	0.9898, *n* value = 0.365
PTX-loaded liposomes (pH 7.4)	0.8945	0.9945	0.9869	0.9879, *n* value = 0.384
PTX-loaded PEG-SpH liposomes (pH 5.5)	0.8226	0.9964	0.9657	0.9851, *n* value = 0.353
PTX-loaded PEG-SpH liposomes (pH 7.4)	0.9901	0.8711	0.9785	0.9699, *n* value = 0.504

and PTX-loaded PEG-SpH liposomes exhibited first-order release kinetics with r^2 values of 0.9904 and 0.9964 respectively (Fig. 5a and c). This suggests that the release of PTX from these formulations followed a process where the drug release rate is directly proportional to the amount of drug remaining in the liposomes [69]. This could be attributed to the pH-sensitive nature of the formulations, which facilitates drug release under acidic conditions mimicking the tumor microenvironment. However, at pH 7.4, the release kinetics diverged between the two formulations. While PTX-loaded liposomes continued to follow first-order release kinetics (r^2 value of 0.9945) (Fig. 5b), PTX-loaded PEG-SpH liposomes exhibited zero-order release kinetics (r^2 value of 0.9901) (Fig. 5d). Zero-order release implies a constant rate of drug release over time, regardless of the remaining drug concentration within the liposomes [70]. This unexpected behavior could be attributed to the altered stability or swelling properties of the PEG-SpH liposomes under physiological pH conditions, with CHEMS ionizing at high pH proving stability leading to a more controlled and sustained release of PTX. The inclusion of mPEG-PCL in our formulation is also particularly noteworthy, as it could contribute to achieving zero-order release. By providing steric stabilization and gradual degradation of the liposomal structure, mPEG-PCL could facilitate the controlled and sustained release of PTX [71]. As per Korsmeyer Peppas fittings, PTX-loaded

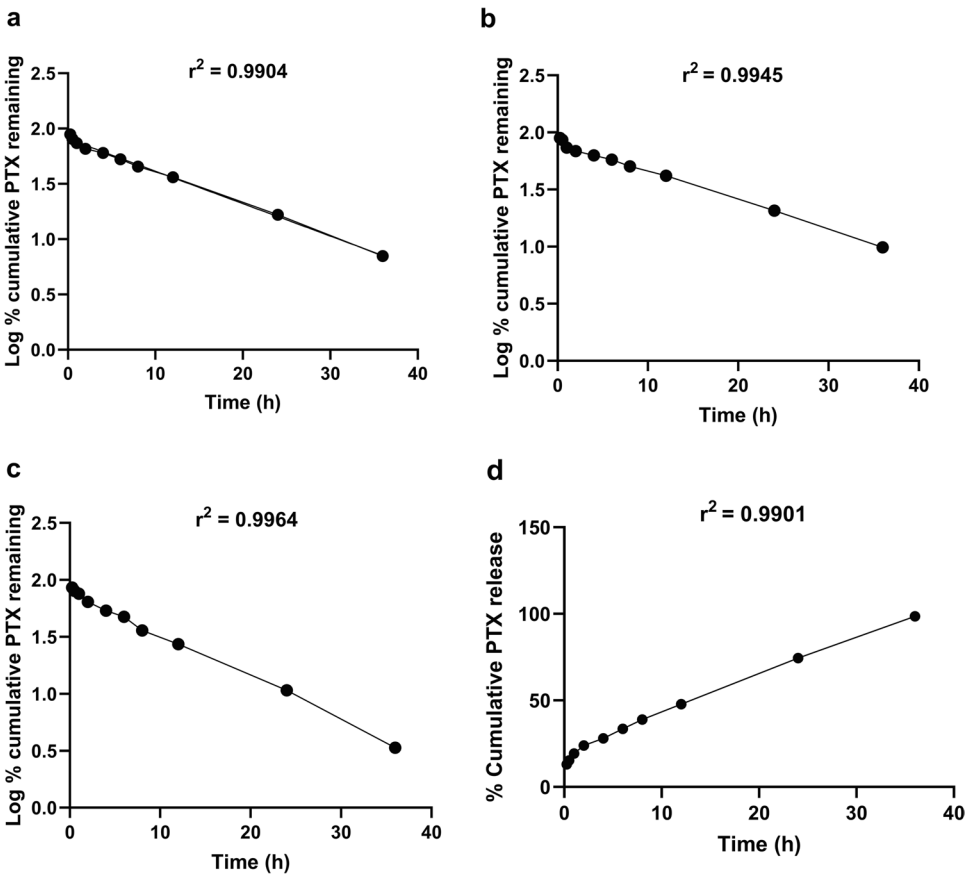

Fig. 5 *In-vitro* release kinetic models fittings: First order release kinetics by **a** PTX-loaded liposomes at pH 5.5, **b** PTX-loaded PEG-SpH liposomes at pH 5.5, **c** PTX-loaded liposomes at pH 7.4 and **d**) PTX-loaded PEG-SpH liposomes at pH 7.4

liposomes at pH 5.5 and 7.4, as well as PTX-loaded PEG-SpH liposomes at pH 5.5 followed the Fickian diffusion-controlled release (≤ 0.45) mechanism with Korsmeyer-Peppas exponent (n value) of 0.365, 0.384, and 0.353 respectively [72]. However, PTX-loaded PEG-SpH liposomes at pH 7.4 displayed a non-Fickian (anomalous) release behavior, with an n value of 0.504 [16]. This behavior could be attributed to the liposomal structure's swelling, erosion, and polymer relaxation, compounded by complex PTX-liposome interactions and hydrodynamic conditions. Additionally, the presence of mPEG-PCL further influences release kinetics by providing steric stabilization and gradual degradation of the liposomal structure.

Quantitative Cellular Uptake Studies on MCF-7 Breast Cancer Cell Line

The quantitative cellular uptake studies were conducted on the MCF-7 breast cancer cell line to assess the uptake efficiency of different formulations: PTX-solution, PTX-loaded liposomes, and PTX-loaded PEG-SpH liposomes. The fluorescence units obtained for PTX-solution, PTX-loaded liposomes, and PTX-loaded PEG-SpH liposomes were 7832.36 ± 742.88, $23{,}894.78 \pm 1257.91$, and $57{,}364.46 \pm 1347.11$, respectively as shown in Fig. 6. These results indicate a significant increase (p-value < 0.001) in cellular uptake of PTX when delivered via liposomal formulations compared to PTX-solution alone. Notably, PTX-loaded PEG-SpH liposomes exhibited the highest cellular uptake, with fluorescence units more than seven times greater than PTX-loaded liposomes and over twenty times greater than PTX-solution. The enhanced uptake efficiency observed with liposomal formulations in comparison to PTX-solution can be attributed to several factors. Liposomes primarily function as a versatile delivery system, protecting PTX from degradation while aiding its targeted delivery to cancer cells [73]. The lipid bilayer structure of liposomes allows them to merge with cellular membranes via endocytosis, facilitating direct transfer of PTX into the cytoplasm [64]. This method of cellular uptake is more effective compared to the passive diffusion seen with free drugs, such as PTX solution, crossing the cell membrane. Additionally, the inclusion of mPEG-PCL in liposomal formulations extends their circulation time in the bloodstream by decreasing recognition and clearance by the reticuloendothelial system (RES) [29, 74]. This extended exposure of liposomes to cancer cells enhances the likelihood of cellular uptake. Additionally, the modification with mPEG-PCL improves the stability of liposomes and enhances their accumulation in tumor tissues via the enhanced permeability and retention (EPR) effect, further boosting cellular uptake efficiency [71]. Furthermore, CHEMS plays a critical role in enhancing cellular uptake through pH-sensitive mechanisms. In the acidic pH environment typical of the tumor microenvironment (pH 5.5), CHEMS undergoes ionization, leading to the destabilization of the liposomal membrane [67] and facilitating the release of encapsulated PTX within cancer cells. This pH-triggered release mechanism enhances the cytotoxic effects of liposomal formulations specifically in the tumor microenvironment, while minimizing off-target effects on healthy tissues [75].

In-vitro Cytotoxicity Studies on MCF-7 Breast Cancer Cell Line

The cytotoxicity of PTX-loaded liposomes and PTX-loaded PEG-SpH liposomes, compared to PTX-solution, was evaluated on the MCF-7 breast cancer cell line after 24 h, 48 h, and 72 h of incubation. The graphical plots of % cell viability and IC_{50} values for formulated liposome formulation are represented in Fig. 7. After 24 h, dose-dependent decreases in cell viability were observed for all formulations. Notably, both PTX-loaded liposomes and PTX-loaded PEG-SpH liposomes exhibited greater cytotoxic effects

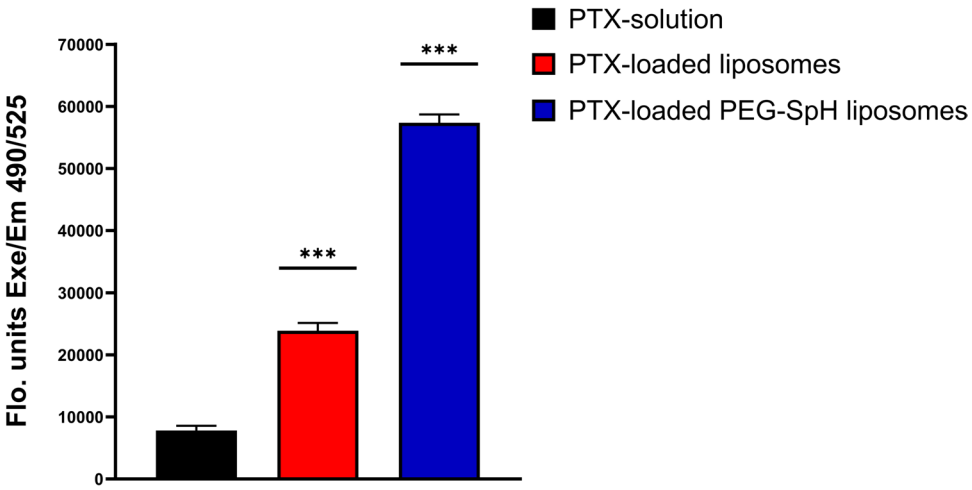

Fig. 6 Quantitative cellular uptake studies on MCF-7 cells. Cell lysate Ex/Em 490/525 nm. Data represented as mean ± SD ($n = 3$). (*** p-value < 0.001 when compared with PTX-solution)

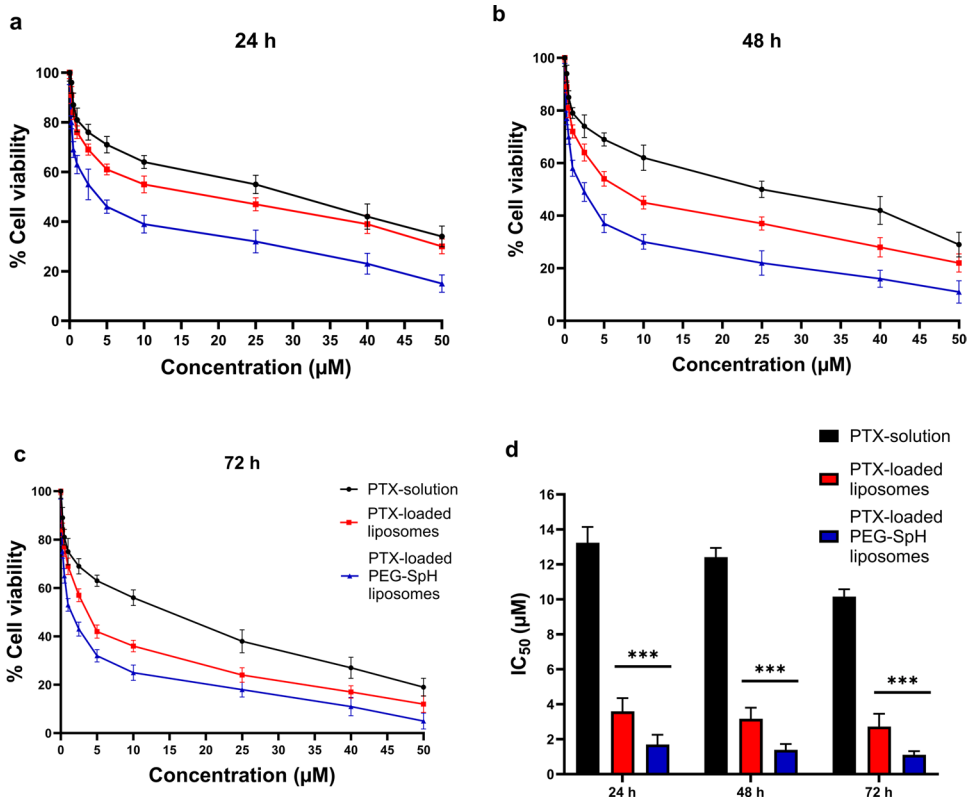

Fig. 7 % cell viability of MCF-7 breast cancer cells after treatment with PTX-loaded liposomes and PTX-loaded PEG-SpH liposomes at **a** 24 h, **b** 48 h, and **c** 72 h as well as **d** summarized IC_{50} values. Data represented as mean ± SD ($n = 6$). (*** p-value < 0.001 when compared with PTX-solution)

compared to PTX-solution. At the highest concentration (50 μM), PTX-solution resulted in 34.67% cell viability, while PTX-loaded liposomes and PTX-loaded PEG-SpH liposomes achieved 30.28% and 15.14%, respectively (Fig. 7a). Furthermore, a significantly improved cytotoxic effect was demonstrated by PTX-loaded liposomes and PTX-loaded PEG-SpH liposomes, supported by IC_{50} values of 3.594 and 1.699 μM respectively in comparison to PTX-solution (p-value < 0.001) (Fig. 7d). Similarly, after 48 h, PTX-solution resulted in 29.31% cell viability, while PTX-loaded liposomes and PTX-loaded PEG-SpH liposomes achieved 22.03% and 11.52%, respectively at the 50 μM concentration (Fig. 7b). The IC_{50} values were also significantly better (p-value < 0.001) for PTX-loaded liposomes and PTX-loaded PEG-SpH liposomes at 3.171 and 1.398 μM respectively (Fig. 7d). Lastly, after 72 h, PTX-loaded liposomes and PTX-loaded PEG-SpH liposomes achieved 12.66% and 5.38% cell viability, respectively, at the 50 μM concentration (Fig. 7c). The IC_{50} values were also significantly better (p-value < 0.001) for PTX-loaded liposomes and PTX-loaded PEG-SpH liposomes at 2.729 and 1.107 μM, respectively (Fig. 7d). These results indicate the sustained and potent cytotoxic effects of both liposomal formulations over an extended incubation period, further highlighting their potential for breast cancer therapy. Overall, the synergistic effects of CHEMS and mPEG-PCL contributed to the enhanced cellular uptake and intracellular drug delivery, thereby improving the cytotoxicity of PTX-loaded PEG-SpH liposomes against MCF-7 breast cancer cells.

Stability Studies

The stability of PTX-loaded PEG-SpH liposomes was evaluated based on changes in particle size, PDI, zeta potential, and encapsulation efficiency over the 4 weeks. At 4°C, particle size increased from 199.25 nm to 219.51 nm by week 4. Similarly, at 25°C, size rose from 199.25 nm to 211.2 nm, while at 37°C, it reached 223.58 nm as seen in Fig. 8(a). Despite temperature variations, changes remained modest, indicating overall stability. These findings suggest temperature influences particle growth, with higher temperatures accelerating this process [76]. However, the formulation demonstrated resilience, maintaining particle integrity across varying storage conditions. For zeta potential, at 4°C, the initial value was -36.94 mV, decreasing to -29.47 mV by week 4. Similarly, at 25°C, it decreased from -36.94 mV to -28.71 mV over the same period, while at 37°C, it showed a more significant decrease from -36.94 mV to -13.47 mV as seen in Fig. 8(b). These fluctuations indicate temperature-dependent changes in zeta potential, with higher temperatures causing more pronounced decreases. However, conventional storage conditions typically do not include

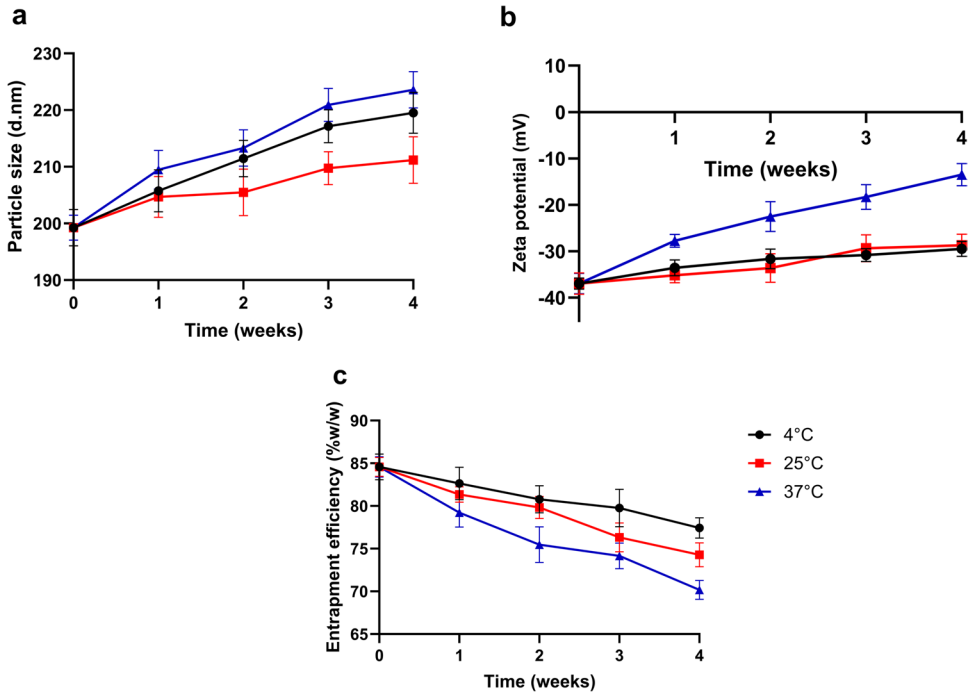

Fig. 8 Influence of storage temperature on **a** Particle size, **b** Zeta potential, and **c** Encapsulation efficiency of PTX-loaded PEG-SpH liposomes. The liposome formulations were stored at 4, 25, and 37°C for 4 weeks. Data represented as mean ± SD ($n = 3$)

temperatures as high as 37°C. Therefore, the observed changes in zeta potential at this elevated temperature may not reflect typical storage conditions but rather provide insight into extreme temperature effects. For encapsulation efficiency, at 4°C, the initial value was 84.57% w/w, gradually decreasing to 77.42% w/w by week 4. Similarly, at 25°C, it decreased from 84.57% w/w to 74.29% w/w over the same period, while at 37°C, it showed a more significant decrease from 84.57% w/w to 70.18% w/w as observed in Fig. 8(c). These trends suggest temperature-dependent changes in encapsulation efficiency, with higher temperatures leading to more pronounced decreases. The stability observed at lower temperatures, such as 4°C and 25°C, with relatively minor decreases in encapsulation efficiency, can be attributed to the slower rates of molecular mobility and degradation processes at these cooler temperatures [77]. At lower temperatures, there is a decrease in molecular mobility, leading to the liposomal structure probably remaining more intact, thereby preserving the encapsulated drug within the vesicles for an extended period and preventing drug leakage or degradation. Conversely, higher temperatures, like 37°C, heighten molecular motion and thermal energy, potentially resulting in more significant disturbances in the liposomal structure [78]. This increased thermal energy can destabilize the lipid bilayer, resulting in increased drug leakage or degradation from the liposomes. As a result, at higher temperatures, the drug's encapsulation efficiency decreases more rapidly due to the elevated chance of drug release or degradation from the liposomal carrier.

Conclusion

In conclusion, this study successfully formulated PTX-loaded PEGylated pH-sensitive liposomes, demonstrating their potential as efficient drug delivery systems for breast cancer treatment. Notably, the pH-sensitive properties were evident, with liposomes exhibiting size variations and zeta potential shifts in response to acidic conditions, enhancing drug release at tumor sites while maintaining stability in physiological environments. At pH 5.5, liposomes showed increased particle size and a shift towards positive zeta potential due to the CHEMS response to acidic conditions. On the other hand, at pH 7.4, a slightly larger size (199.25 nm) and more negative zeta potential (-36.94 mV) were observed. Quantitative cellular uptake studies demonstrated enhanced PTX internalization, with fluorescence units of 57,364.46 obtained for PTX-loaded PEG-SpH liposomes, highlighting the role of mPEG-PCL in prolonging circulation time and CHEMS in facilitating drug release within the tumor microenvironment. Moreover, PTX-loaded PEG-SpH liposomes exhibited significantly improved cytotoxicity against MCF-7 breast cancer cells compared to plain PTX-solution, with an IC_{50} value of 1.107 µM, approximately 90% lower than plain PTX-solution, underscoring their potential for enhanced therapeutic outcomes. Stability studies further confirmed the robustness of the liposomal formulation under various storage conditions, emphasizing their suitability for clinical applications. Overall, these findings show the promise of PEGylated pH-responsive liposomes as versatile nanocarriers for optimizing PTX

therapy against breast cancer, offering targeted drug delivery, enhanced cellular uptake, and improved cytotoxicity. Further research is warranted to explore their clinical translation and potential combination therapies for improved efficacy and patient outcomes in breast cancer treatment.

Supplementary Information The online version contains supplementary material available at https://doi.org/10.1208/s12249-024-02930-7.

Acknowledgements The author(s) would like to thank Dr. Arun Kedia, VAV Life Sciences Pvt Ltd (Mumbai, India) for providing Leciva S-90. The author(s) would also like to thank Cipla Ltd. (Mumbai, India) for the generous gift sample of Paclitaxel.

Author Contributions Harsh P. Nijhawan: conceptualization, methodology, investigation, writing, reviewing, and editing the final manuscript.

Pooja Shyamsundar: methodology, investigation, writing original draft.

Bala Prabhakar: conceptualization, validation, supervision.

Khushwant S. Yadav: conceptualization, validation, supervision.

Funding The author(s) reported there is no funding associated with the work featured in this article.

Data Availability Data is contained within the article. Any additional data will be made available on request.

Declarations

Conflict of Interest The author(s) declare no conflict of interest.

References

1. Siegel Mph RL, Miller KD, Sandeep N, Mbbs W, Ahmedin J, Dvm J, et al. Cancer statistics, 2023. CA Cancer J Clin. 2023;73:17–48.
2. Buchheit JT, Schacht D, Kulkarni SA. Update on management of ductal carcinoma in situ. Clin Breast Cancer. 2023. https://doi.org/10.1016/j.clbc.2023.12.010.
3. El Saghir NS, Tfayli A, Hatoum HA, Nachef Z, Dinh P, Awada A. Treatment of metastatic breast cancer: State-of-the-art, subtypes and perspectives. Crit Rev Oncol Hematol. 2011;80:433–49.
4. Sun M, Gao Y, Zhu Z, Wang H, Han C, Yang X, et al. A systematic in vitro investigation on poly-arginine modified nanostructured lipid carrier: Pharmaceutical characteristics, cellular uptake, mechanisms and cytotoxicity. Asian J Pharm Sci. 2017;12:51–8.
5. Maksimovic-Ivanic D, Fagone P, McCubrey J, Bendtzen K, Mijatovic S, Nicoletti F. HIV-protease inhibitors for the treatment of cancer: Repositioning HIV protease inhibitors while developing more potent NO-hybridized derivatives? Int J Cancer. 2017;140:1713–26.
6. Koudelka Š, Turánek J. Liposomal paclitaxel formulations. J Control Release. 2012;163:322–34.
7. Zhang JA, Anyarambhatla G, Ma L, Ugwu S, Xuan T, Sardone T, et al. Development and characterization of a novel Cremophor® EL free liposome-based paclitaxel (LEP-ETU) formulation. Eur J Pharm Biopharm. 2005;59:177–87.
8. Singh S, Dash AK. Paclitaxel in Cancer Treatment: Perspectives and Prospects of its Delivery Challenges. Crit Rev Trade Ther Drug Carrier Syst. 2009;26:333–72.
9. Gavas S, Quazi S, Karpiński TM. Nanoparticles for Cancer Therapy: Current Progress and Challenges. Nanoscale Res Lett. 2021;16:1–21.
10. Raut H, Jadhav C, Shetty K, Laxane N, Nijhawan HP, Rao GK, et al. Sorafenib tosylate novel drug delivery systems: Implications of nanotechnology in both approved and unapproved indications. OpenNano. 2022;8:100103.
11. Filipczak N, Pan J, Yalamarty SSK, Torchilin VP. Recent advancements in liposome technology. Adv Drug Deliv Rev. 2020;156:4–22.
12. Deshpande PP, Biswas S, Torchilin VP. Current trends in the use of liposomes for tumor targeting. Nanomedicine (Lond). 2013;8:1509–28.
13. Wang L. Preparation and in vitro evaluation of an acidic environment-responsive liposome for paclitaxel tumor targeting. Asian J Pharm Sci. 2017;12:470–7.
14. Milligan JJ, Saha S. A nanoparticle's journey to the tumor: Strategies to overcome first-pass metabolism and their limitations. Cancers. 2022;14:1741.
15. Nakamura K, Yamashita K, Itoh Y, Yoshino K, Nozawa S, Kasukawa H. Comparative studies of polyethylene glycol-modified liposomes prepared using different PEG-modification methods. Biochim Biophys Acta (BBA) - Biomembr. 2012;1818:2801–7.
16. Bhargave H, Nijhawan H, Yadav KS. PEGylated Erlotinib HCl Injectable Nanoformulation for Improved Bioavailability. AAPS PharmSciTech. 2023;24. https://doi.org/10.1208/s12249-023-02560-5.
17. Fam SY, Chee CF, Yong CY, Ho KL, Mariatulqabtiah AR, Tan WS. Stealth coating of nanoparticles in drug-delivery systems. Nanomaterials. 2020;10:787.
18. Hussain Z, Khan S, Imran M, Sohail M, Shah SWA, de Matas M. PEGylation: a promising strategy to overcome challenges to cancer-targeted nanomedicines: a review of challenges to clinical transition and promising resolution. Drug Deliv Transl Res. 2019;9:721–34.
19. Danhier F, Feron O, Préat V. To exploit the tumor microenvironment: Passive and active tumor targeting of nanocarriers for anticancer drug delivery. J Control Release. 2010;148:135–46.
20. Nijhawan HP, Prabhakar B, Misra A, Yadav KS. Fragmented antibodies in non-small cell lung cancer: A novel nano-engineered delivery system for detection and treatment of cancer. Drug Discov Today. 2023;28:103701.
21. Wang J, Gong J, Wei Z. Strategies for Liposome Drug Delivery Systems to Improve Tumor Treatment Efficacy. AAPS PharmSciTech. 2021;23:1–14.
22. Kraft JC, Freeling JP, Wang Z, Ho RJY. Emerging Research and Clinical Development Trends of Liposome and Lipid Nanoparticle Drug Delivery Systems. J Pharm Sci. 2014;103:29–52.
23. Alrbyawi H, Poudel I, Annaji M, Boddu SHS, Arnold RD, Tiwari AK, et al. pH-Sensitive liposomes for enhanced cellular uptake and cytotoxicity of daunorubicin in melanoma (B16-BL6) cell lines. Pharmaceutics. 2022;14:1128.
24. Fan Y, Chen C, Huang Y, Zhang F, Lin G. Study of the pH-sensitive mechanism of tumor-targeting liposomes. Colloids Surf B Biointerfaces. 2017;151:19–25.
25. Yessine MA, Leroux JC. Membrane-destabilizing polyanions: interaction with lipid bilayers and endosomal escape of biomacromolecules. Adv Drug Deliv Rev. 2004;56:999–1021.
26. Paliwal SR, Paliwal R, Vyas SP. A review of mechanistic insight and application of pH-sensitive liposomes in drug delivery. Drug Deliv. 2015;22:231–42.
27. Zhai Y, Zhou X, Zhang Z, Zhang L, Wang D, Wang X, et al. Design, synthesis, and characterization of schiff base bond-linked pH-responsive doxorubicin prodrug based on functionalized mPEG-PCL for targeted cancer therapy. Polymers. 2018;10:1127.

28. Hani U, Rahamathulla M, Osmani RA, Kumar HY, Urolagin D, Ansari MY, et al. Recent advances in novel drug delivery systems and approaches for management of breast cancer: A comprehensive review. J Drug Deliv Sci Technol. 2020;56:101505.
29. Bhargave H, Nijhawan H, Yadav KS. PEGylated Erlotinib HCl Injectable Nanoformulation for Improved Bioavailability. AAPS PharmSciTech [Internet]. 2023 [cited 2024 Mar 24];24. Available from: https://pubmed.ncbi.nlm.nih.gov/37038015/.
30. Aryasomayajula B, Salzano G, Torchilin VP. Multifunctional liposomes. Methods Mol Biol. 2017;1530:41–61.
31. Yadav KS, Raut HC, Nijhawan HP. Inhalable spray-dried polycaprolactone-based microparticles of Sorafenib Tosylate with promising efficacy on A549 cells. Pharm Dev Technol. 2023;28:755–67.
32. Kass B, Schemmert S, Zafiu C, Pils M, Bannach O, Kutzsche J, et al. Aβ oligomer concentration in mouse and human brain and its drug-induced reduction ex vivo. Cell Rep Med. 2022;3:100630.
33. Jang E, Lim EK, Choi Y, Kim E, Kim HO, Kim DJ, et al. π-Hyaluronan nanocarriers for CD44-targeted and pH-boosted aromatic drug delivery. J Mater Chem B. 2013;1:5686–93.
34. Nguyen TL, Nguyen TH, Nguyen DH. Development and in vitro evaluation of liposomes using soy lecithin to encapsulate paclitaxel. Int J Biomater. 2017;2017:1.
35. Yadav KS, Sawant KK. Modified nanoprecipitation method for preparation of cytarabine-loaded PLGA nanoparticles. AAPS PharmSciTech. 2010;11:1456.
36. Wu IY, Bala S, Škalko-Basnet N, di Cagno MP. Interpreting non-linear drug diffusion data: Utilizing Korsmeyer-Peppas model to study drug release from liposomes. Eur J Pharm Sci. 2019;138:105026.
37. Ritger PL, Peppas NA. A simple equation for description of solute release. II Fickian and anomalous release from swellable devices. J Control Release. 1987;5:37–42.
38. Peppas NA. Analysis of Fickian and non-Fickian drug release from polymers. Pharm Acta Helv. 1985;60:110–1.
39. Paarakh MP, Jose PA, Setty C, Peterchristoper GV. Release kinetics – Concepts and applications. Int J Pharm Res Technol (IJPRT). 2018;8:12–20.
40. Shi C, Gao F, Gao X, Liu Y. A novel anti-VEGF165 monoclonal antibody-conjugated liposomal nanocarrier system: Physical characterization and cellular uptake evaluation in vitro and in vivo. Biomed Pharmacother. 2015;69:191–200.
41. Yadav KS, Jacob S, Sachdeva G, Chuttani K, Mishra AK, Sawant KK. Long circulating PEGylated PLGA nanoparticles of cytarabine for targeting leukemia. J Microencapsul. 2011;28:729–42.
42. Kale K, Fulfager A, Juvale K, Yadav KS. Long circulating polymeric nanoparticles of gemcitabine HCl using PLGA-PEG-PPG-PEG block co-polymer. Int J Polym Mater Polym Biomater. 2024;73:176–89.
43. Le TVT, Suh JH, Kim N, Park HJ. In silico identification of poly(ADP-ribose)polymerase-1 inhibitors and their chemosensitizing effects against cisplatin-resistant human gastric cancer cells. Bioorg Med Chem Lett. 2013;23:2642–6.
44. Carrillo-Castillo TD, Castro-Carmona JS, Luna-Velasco A, Zaragoza-Contreras EA. PH-responsive polymer micelles for methotrexate delivery at tumor microenvironments. E-Polymers. 2020;20:624–35.
45. Verma P, Yadav KS. Quality by Design (QbD) enabled and Box-Behnken design assisted approach for formulation of tranexamic acid loaded stratum corneum lipid liposomes. J Drug Deliv Sci Technol. 2023;86:104571.
46. Verma P, Singh RK, Wadhwa A, Prabhakar B, Yadav KS. Bimatoprost-loaded lipidic nanoformulation development using quality by design: liposomes versus solid lipid nanoparticles in intraocular pressure reduction. Nanomedicine. 2023;18:1815–37. https://doi.org/10.2217/nnm-2023-0141.
47. Tarantash M, Nosrati H, Kheiri Manjili H, Baradar KA. Preparation, characterization and in vitro anticancer activity of paclitaxel conjugated magnetic nanoparticles. Drug Dev Ind Pharm. 2018;44:1895–903.
48. Son SR, An J, Choi JW, Park J, Park CB, Lee JH. Hierarchical self-constructed biomolecular nanolayers comprising cholesterol and cholesteryl hemisuccinate for automatic alignment of liquid crystals. J Mol Liq. 2021;340:116842.
49. Khashi M, Hassanajili S, Golestaneh SI. Electrospun poly-lactic acid/chitosan nanofibers loaded with paclitaxel for coating of a prototype polymeric stent. Fibers Polym. 2018;19:1444–53.
50. Caddeo C, Pucci L, Gabriele M, Carbone C, Fernàndez-Busquets X, Valenti D, et al. Stability, biocompatibility and antioxidant activity of PEG-modified liposomes containing resveratrol. Int J Pharm. 2018;538:40–7.
51. Davoodi P, Lee LY, Xu Q, Sunil V, Sun Y, Soh S, et al. Drug delivery systems for programmed and on-demand release. Adv Drug Deliv Rev. 2018;132:104–38.
52. Moghimi SM, Hedeman H, Christy NM, Illum L, Davis SS. Enhanced hepatic clearance of intravenously administered sterically stabilized microspheres in zymosan-stimulated rats. J Leukoc Biol. 1993;54:513–7.
53. Driscoll DF. Globule-size distribution in injectable 20% lipid emulsions: Compliance with USP requirements. Am J Health Syst Pharm. 2007;64:2032–6.
54. Steichen SD, Caldorera-Moore M, Peppas NA. A review of current nanoparticle and targeting moieties for the delivery of cancer therapeutics. Eur J Pharm Sci. 2013;48:416.
55. Ernsting MJ, Murakami M, Roy A, Li SD. Factors controlling the pharmacokinetics, biodistribution and intratumoral penetration of nanoparticles. J Control Release. 2013;172:782–94.
56. Campos FL, de Alcântara Lemos J, Oda CMR, de Oliveira Silva J, Fernandes RS, Miranda SEM, et al. Irinotecan-loaded polymeric micelles as a promising alternative to enhance antitumor efficacy in colorectal cancer therapy. Polymers. 2022;14:4905.
57. Kanamala M, Wilson WR, Yang M, Palmer BD, Wu Z. Mechanisms and biomaterials in pH-responsive tumour targeted drug delivery: A review. Biomaterials. 2016;85:152–67.
58. Ganta S, Devalapally H, Shahiwala A, Amiji M. A review of stimuli-responsive nanocarriers for drug and gene delivery. J Control Release. 2008;126:187–204.
59. Kono K, Zenitani K, Takagishi T. Novel pH-sensitive liposomes: liposomes bearing a poly(ethylene glycol) derivative with carboxyl groups. Biochim Biophys Acta (BBA) - Biomembr. 1994;1193:1–9.
60. Liu X, Huang G. Formation strategies, mechanism of intracellular delivery and potential clinical applications of pH-sensitive liposomes. Asian J Pharm Sci. 2013;8:319–28.
61. Jayapriya P, Pardhi E, Vasave R, Guru SK, Madan J, Mehra NK. A review on Stimuli-pH responsive liposomal formulation in cancer therapy. J Drug Deliv Sci Technol. 2023;90:105172.
62. Hafez IM, Cullis PR. Cholesteryl hemisuccinate exhibits pH sensitive polymorphic phase behavior. Biochim Biophys Acta Biomembr. 2000;1463:107–14.
63. Danafar H, Davaran S, Rostamizadeh K, Valizadeh H, Hamidi M. Biodegradable m-PEG/PCL core-shell micelles: preparation and characterization as a sustained release formulation for curcumin. Adv Pharm Bull. 2014;4:501.
64. Lee Y, Thompson DH. Stimuli-responsive liposomes for drug delivery. Wiley Interdiscip Rev Nanomed Nanobiotechnol. 2017;9:e1450.
65. Franco MS, Gomes ER, Roque MC, Oliveira MC. Triggered drug release from liposomes: exploiting the outer and inner tumor environment. Front Oncol. 2021;11:623760.

66. Jo SM, Xia Y, Lee HY, Kim YC, Kim JC. Liposomes incorporating hydrophobically modified glucose oxidase. Korean J Chem Eng. 2008;25:1221–5.
67. Jo SM, Lee HY, Kim JC. Glucose-sensitive liposomes incorporating hydrophobically modified glucose oxidase. Lipids. 2008;43:937–43.
68. Shah H, Madni A, Khan MM, Ahmad FUD, Jan N, Khan S, et al. pH-responsive liposomes of dioleoyl phosphatidylethanolamine and cholesteryl hemisuccinate for the enhanced anticancer efficacy of cisplatin. Pharmaceutics. 2022;14:129.
69. Jain A, Jain SK. In vitro release kinetics model fitting of liposomes: An insight. Chem Phys Lipids. 2016;201:28–40.
70. Maritim S, Boulas P, Lin Y. Comprehensive analysis of liposome formulation parameters and their influence on encapsulation, stability and drug release in glibenclamide liposomes. Int J Pharm. 2021;592:120051.
71. Mohanty C, Acharya S, Mohanty AK, Dilnawaz F, Sahoo SK. Curcumin-encapsulated MePEG/PCL diblock copolymeric micelles: a novel controlled delivery vehicle for cancer therapy. Nanomedicine. 2010;5:433–49. https://doi.org/10.2217/nnm109.
72. Tai K, Rappolt M, He X, Wei Y, Zhu S, Zhang J, et al. Effect of β-sitosterol on the curcumin-loaded liposomes: Vesicle characteristics, physicochemical stability, in vitro release and bioavailability. Food Chem. 2019;293:92–102.
73. Jain A, Jain SK. Advances in tumor targeted liposomes. Curr Mol Med. 2018;18:44–57.
74. Wang Y, Gou M, Gong C, Wang C, Qian Z, Feng Lin Y, et al. Pharmacokinetics and Disposition of nanomedicine using biodegradable PEG/PCL polymers as drug carriers. Curr Drug Metab. 2012;13:338–53.
75. Rathnayake K, Patel U, Hunt EC, Singh N. Fabrication of a dual-targeted liposome-coated mesoporous silica core-shell nanoassembly for targeted cancer therapy. ACS Omega. 2023;8:34481–98.
76. Costa AP, Xu X, Burgess DJ. Freeze-anneal-thaw cycling of unilamellar liposomes: Effect on encapsulation efficiency. Pharm Res. 2014;31:97–103.
77. Sydykov B, Oldenhof H, Sieme H, Wolkers WF. Storage stability of liposomes stored at elevated subzero temperatures in DMSO/sucrose mixtures. PLoS ONE. 2018;13:e0199867.
78. Elizondo E, Moreno E, Cabrera I, Córdoba A, Sala S, Veciana J, et al. Liposomes and Other Vesicular Systems: Structural Characteristics, Methods of Preparation, and Use in Nanomedicine. Prog Mol Biol Transl Sci. 2011;104:1–52.